TIME-DEPENDENT TRAVELING WAVE TUBE MODEL FOR INTERSYMBOL INTERFERENCE INVESTIGATIONS

Carol L. Kory[1] and Monty Andro[2]
[1]Analex Corporation/[2]NASA Glenn Research Center
21000 Brookpark Road, MS 54-5
Cleveland, OH 44135
Carol.L.Kory@grc.nasa.gov

Abstract

For the first time, a computational model has been used to provide a direct description of the effects of the TWT on modulated digital signals. The TWT model comprehensively takes into account the effects of frequency dependent AM/AM and AM/PM conversion; gain and phase ripple; drive-induced oscillations; harmonic generation; intermodulation products; and backward waves. Thus, signal integrity can be investigated in the presence of these sources of potential distortion as a function of the physical geometry of the high power amplifier and the operational digital signal. This method promises superior predictive fidelity compared to methods using TWT models based on swept-amplitude and/or swept-frequency data.

The fully three-dimensional (3D), time-dependent, TWT interaction model using the electromagnetic code MAFIA is presented. This model is used to investigate assumptions made in TWT black-box models used in communication system level simulations. In addition, digital signal performance, including intersymbol interference (ISI), is compared using direct data input into the MAFIA model and using the system level analysis tool, SPW.

I. INTRODUCTION

The phenomenal growth of the satellite communications industry has created a large demand for increased data rates, enforcing high-level modulation schemes, larger system bandwidth (BW) and minimum distortion of the modulated signal as it is passed through the traveling wave tube amplifier (TWTA). As more complex modulation and multiple access techniques are employed, ISI becomes a major consideration for accurate data detection at the receiver. It is suspected that in addition to the dispersion of the TWT, frequency dependent reflections due to mismatches within the TWT are a significant contributor to ISI. To experimentally investigate the effect of these mismatches within the physical TWT on ISI would be prohibitively expensive, as it would require manufacturing numerous amplifiers in addition to the acquisition of the required digital hardware.

Standard practice involves using communication system level software to predict if adequate signal detection will be achieved. These models use a nonlinear, black box model to represent the TWTA. Currently, SPW [1] is used in-house at NASA Glenn Research Center (GRC), where the behavior of the TWTA is characterized by a memoryless envelope model. The model parameters are obtained from the AM/AM (output power versus input power) and AM/PM (output phase versus input power) conversions, which are typically obtained by sweeping the input amplitude at the center frequency either experimentally or by using conventional frequency domain TWT codes such as TWA3 [2]. Thus, the TWT characteristics are assumed constant (memoryless) over the bandwidth of the simulated signal. In addition, the model does not account for the memory effects of signal reflections occurring within the TWT. As data rate requirements increase and complex, wide-band, digital signals are employed, the assumptions made in conventional system level modeling become less accurate.

A fully 3D, time-dependent, TWT interaction model has been developed [3] using the electromagnetic particle-in-cell (PIC) code MAFIA (Solution of MAxwell's equations by the Finite-Integration-Algorithm) [4, 5]. This physics based TWT model can be used to give a direct description of the effects of the nonlinear TWT on the operational signal as a function of the physical device. The actual geometry of the device is taken into account as the user can define arbitrary slow-wave circuits, input/output coupling, and beam focusing structures allowing standard or novel TWT's to be investigated. Because the model is 3D, the geometry is not limited to azimuthally symmetric structures. The user is also able to define arbitrary excitation functions so that modulated digital signals can be used as input and computational correlation of ISI with TWT parameters can be directly conducted.

Additionally, the MAFIA time-dependent data can be used as input to develop system level, nonlinear, black box models for the TWT with memory such as in [6], where experimental data is currently used to obtain model parameters. This type of system level nonlinear model can be expected to possess superior predictive fidelity compared to models based on swept-tone, swept-amplitude data. The latter data is partial because superposition does not apply in the nonlinear device, and the interactions between frequency components in a realistic signal are not captured [7].

II. MAFIA TWT MODEL

The TWT used as a model for this study is a Northrop Grumman, 2-6 GHz TWT designated the XWING (eXperimental WIsconsin Northrop Grumman). This TWT includes a rectangular tape, helical, slow-wave circuit. Uniform magnetic focusing is used to contain a

2.8 kV, 0.22 A beam.

The cold-test characteristics of the helical slow-wave circuit were calculated using a single helical turn and the MAFIA eigenmode solver as described in [3]. The simulated normalized phase velocity is compared to measured data in Figure 1 showing an average absolute difference across the frequency band of 0.5 percent.
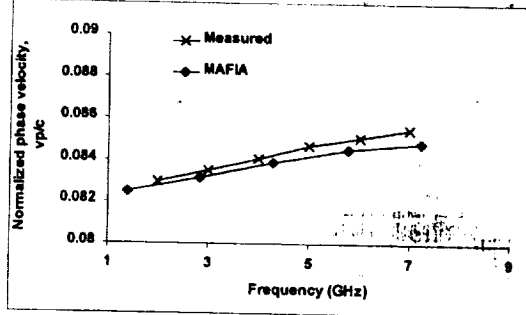

Figure 1 Measured and simulated normalized phase velocity

Next, the helical slow-wave circuit was extended to several helical turns and input/output coupling designed to couple the RF signal in and out of the circuit. The S-parameters were calculated using MAFIA as described in [3], and the return loss is plotted as a function of frequency for the final coupler design in Figure 2. The match is excellent around 4.2 GHz with a return loss of -35 dB. Therefore, we choose this value as our center frequency f_c for all simulations.
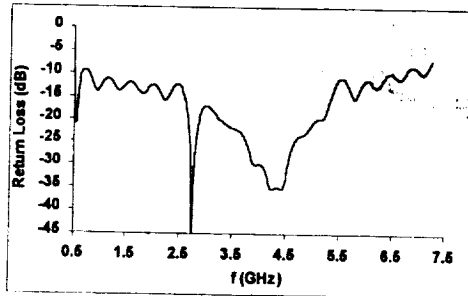

**Figure 2 Return loss for simulated XWING coupler design**

To complete the helical interaction model, an electron beam was defined consistent with the XWING operating parameters, and a static uniform focusing field was implemented. Conductor and dielectric losses were assumed zero in all simulations. Because of the computational intensity added by modeling in 3D, the interaction model was limited to about 40 helical turns. This length corresponds to a small signal gain of 12.5 dB at 4.2 GHz, which we feel is sufficient for this study.

The power transfer characteristics at 4.2 GHz were obtained using both MAFIA and the 2.5D frequency-domain, TWT code TWA3 [2]. The output power and phase shift from small-signal (i.e. AM/AM and AM/PM) as a function of input drive power are shown in Figure 3. The agreement in output power is good at low input drive levels, but worsens near saturation. For this broadband circuit, we found from the MAFIA simulations that the

second harmonic (at 8.4 GHz) is synchronous with the electron beam, and thus experiences gain. Therefore, we attribute the discrepancies to its strength near saturation. The phase plot shows a phase change $\Delta\phi$ between an input power of 30 dB below saturation and saturation of 9.6 and 18.9 degrees for the TWA3 and MAFIA models, respectively.
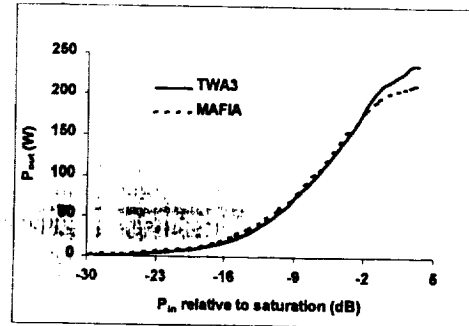
(a)
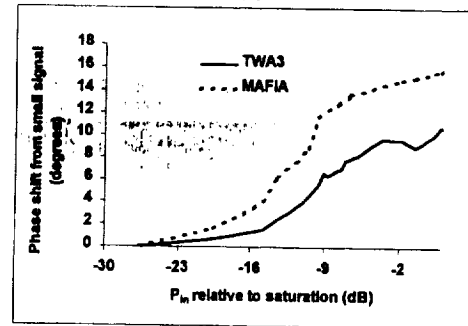
(b)

Figure 3 Simulated (a) output power and (b) phase as a function of input power at 4.2 GHz

III. INVESTIGATION OF SYSTEM LEVEL TWT MODEL ASSUMPTIONS

Conventional system level nonlinear black box models representing the TWTA vary in complexity [7], but most make several assumptions regarding the operation of the high power amplifier. In particular, it is common to neglect the following TWT operational characteristics:

1. Dependence of AM/AM and AM/PM with frequency
2. Effects of reflections and second harmonics
3. Differences between broadband and single-tone excitations
4. Dependence of gain and phase ripples with drive power
5. Dependence of output spectrum with operational signal

The TWTA box model used in SPW does not account for any of these characteristics. The significance of neglecting them is investigated quantitatively in this section using the MAFIA model.

### A. Dependence of AM/AM and AM/PM with frequency

The frequency variation of these parameters is inherently considered in subsequent sections.

B. Effects of reflections and second harmonics

Several single-tone excitations were simulated with MAFIA and the TWT output was recorded at the first arrival of the RF signal at the output port (without reflections), and at a point in time after the signal had time to make one feedback path around the TWT and return to the output port (with reflections). An operating point of 5 dB input backoff (IBO) relative to saturation was chosen as might be used for high data rate communications using multi-level modulation schemes. From here forth, IBO will be specified relative to saturation at 4.2 GHz.
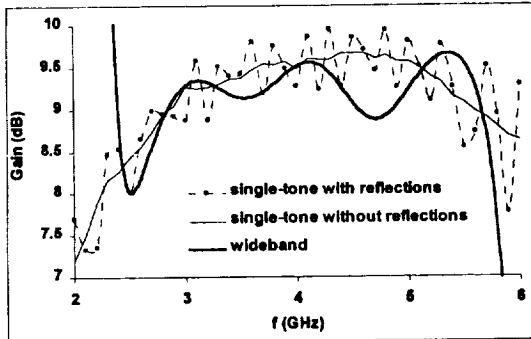
(a)
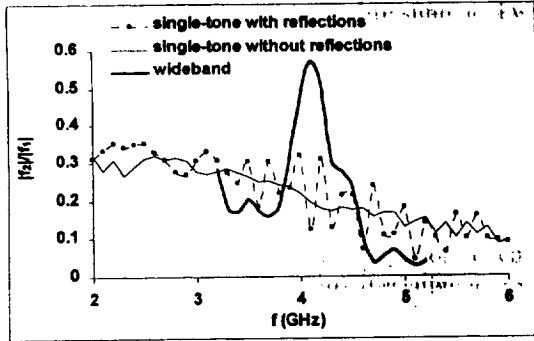
(b)

Figure 4 (a) Gain and (b) relative strength of second harmonic with and without reflections as a function of frequency

Comparisons of the gain and strength of the second harmonic frequency f_2 relative to the fundamental frequency f_1 with and without reflections are shown in Figure 4. The average absolute difference in gain between the two cases is 0.28 dB across the bandwidth. The gain plot for the case with reflections shows a peak-to-peak variation of as much as 0.72 dB around 4.2 GHz. Conventional theory predicts negligible ripple where there are negligible reflections [8]. However, for this circuit the ripple can be attributed to the second harmonic interaction with the beam and its large reflections at the input/output couplers. The average absolute difference in phase across the frequency band is 5.7 degrees.

C. Differences between broadband and single-tone excitations

The TWT characteristics are compared when excited by single-tones versus wideband root raised cosine (RRC) shaped symbols, as would be used to represent realistic

digital symbols [9].

A series of 4 GHz bandwidth symbols were transmitted with average input power at a 5 dB IBO allowing the signal to be repeatedly reflected so it travels the feedback cycle of the TWT several times. The gain and second harmonic strength of the last wideband output symbol are compared to data using single-tone excitation with and without reflections in Figure 4. The overall behaviors are very different for the single-tone and wideband excitations. The plots show that using single-tone excitation data without reflections would incorrectly predict gain by as much as about 1 dB. As the signal at 8.4 GHz is repeatedly reflected, it is also repeatedly amplified attributing to it's strength.

D. Dependence of gain and phase ripples with drive power

Several 2 GHz bandwidth, RRC symbols were simulated with various input powers. Within this bandwidth, the return loss is better than –20 dB across the bandwidth, and there are no second harmonics within the operating band. Thus, it represents a more realistic scenario for communications applications. The normalized output spectrums are shown in Figure 5. A power hole (as much as about one dB at 4.2 GHz) exists in the operating band, increasing with input drive due to the second harmonic strength, which also increases with drive power reaching about 60% of the fundamental near saturation. The gain and phase ripples, shown in Figure 6, were calculated as the maximum deviation of the gain and phase, respectively, for the RRC output symbols. The largest values correspond to the largest IBO and decrease, in general, with increasing drive power. Comparing the gain ripple for the 5.1 IBO data in Figure 6 (a) to that in Figure 4 (a) for single tone excitations further demonstrates the differences in the TWT output as a function of excitation.

E. Dependence of output spectrum with operational signal

To further demonstrate the idea that direct excitation with the operational signal provides superior simulated results, we compare the frequency spectrums of several modulated signals. The bandwidth was kept constant at 2 GHz and the symbols were shaped using a RRC filter with roll off factor $\alpha = 0.3$. Three cases are compared: 1) binary phase shift keying (BPSK), 2) 16-ary quadrature amplitude modulation (16-QAM), and 3) 64-QAM. Figure 7 shows the output spectrum for each excitation. The peak-to average power ratio P_p/P_{avg} and IBO are shown in the figure caption.

IV.   MAFIA AND SPW COMPARISONS

Digital signal performance is compared using direct excitation of the MAFIA model and SPW simulations. The TWT box model used in the SPW simulations uses the MAFIA generated AM/AM and AM/PM data shown in Figure 3 and makes the assumptions listed in Section III.
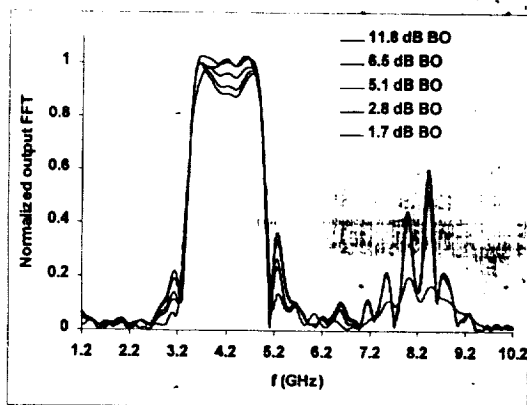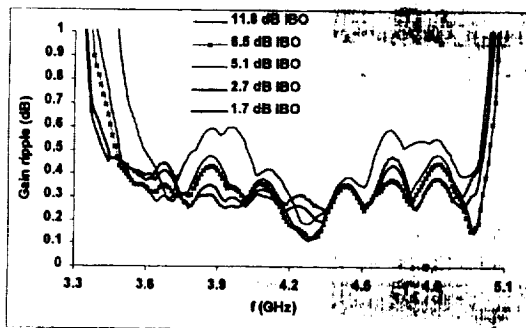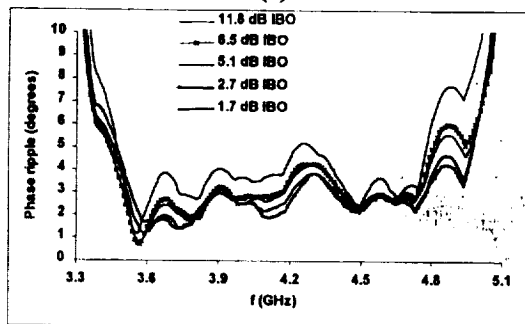
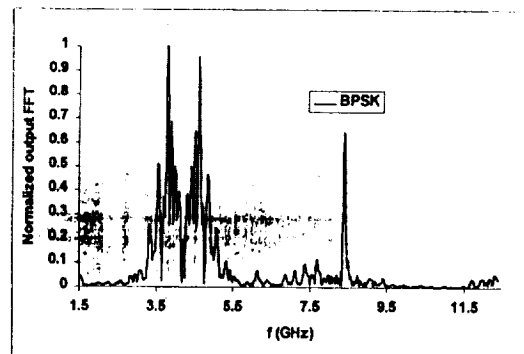**Figure 5 Simulated normalized output spectrum using wideband excitation (BW = 2 GHz)**
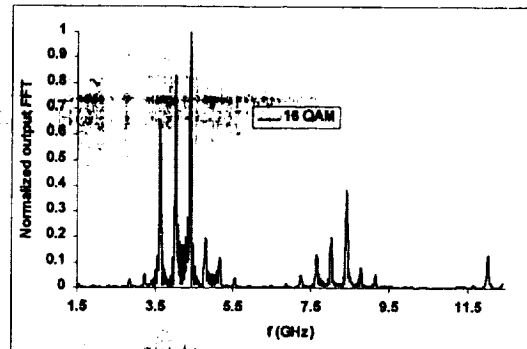

(a)

(b)

Figure 6 (a) Gain and (b) phase ripples using wideband excitation at various levels of input backoff (BW = 2 GHz)

(a)

(b)

(c)

Figure 7 Normalized output spectrum for (a) BPSK (3.1 IBO, P_p/P_{avg} = 4.5 dB), (b) 16-QAM (7.0 IBO, P_p/P_{avg} = 7.0 dB), and (c) 64-QAM (7.1 IBO, P_p/P_{avg} = 7.1 dB) (BW = 2 GHz)

The eye diagram is commonly used to qualitatively measure the degree of distortion due to ISI. Figure 8 shows eye diagrams generated from SPW and MAFIA output for a 2 GHz bandwidth, BPSK signal at a 3.1 dB IBO. The absolute differences in upper bound degradation, which is proportional to the opening of the eye diagram [7], are shown between the SPW and MAFIA simulations as a function of signal bandwidth and IBO in Figure 9. The discrepancies become worse with increased bandwidth (as larger reflections are present), and increased drive powers (as the power hole increases).
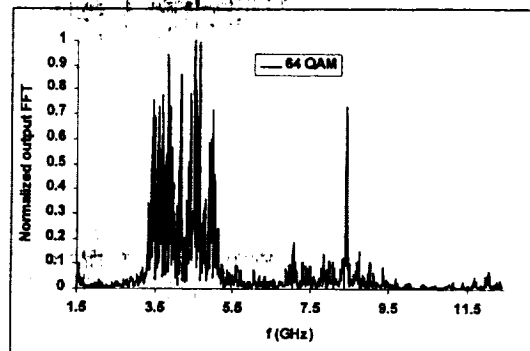
Constellation diagrams showing the output signal amplitude and phase for a 16-QAM signal are compared in Figure 10 (data shown only for second and fourth quadrants). SPW results were identical for 2 and 4 GHz BWs. The upper bound degradation was calculated from

the corresponding eye diagrams (not shown). Compared to SPW simulations, the MAFIA 2 and 4 GHz cases resulted in larger degradations by 1.6 and 3.6 dB, respectively.

V. CONCLUSIONS

Results show significant differences in predicted degradation between SPW and MAFIA simulations. This demonstrates the significance of the approximations made in the SPW model regarding the TWT characteristics, on digital signal performance.

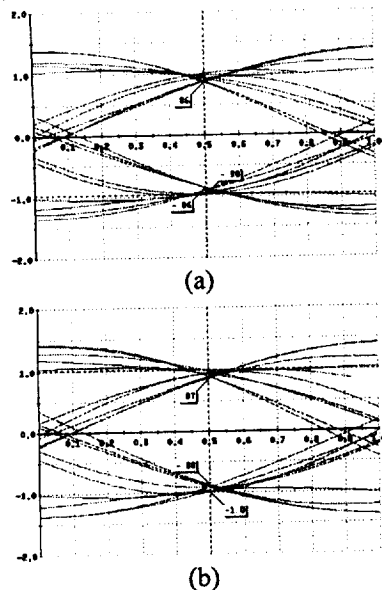Microwave) for his assistance in the coupler design.

(a)

(b)

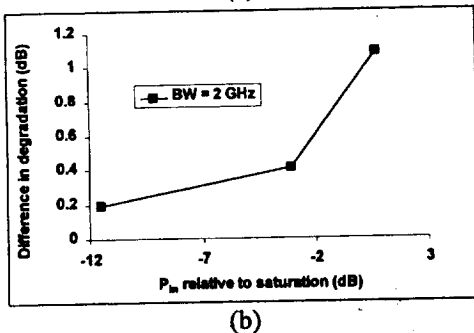**Figure 8 BPSK eye diagrams (BW = 2 GHz, 3.1 dB IBO) (a) SPW (b) MAFIA**
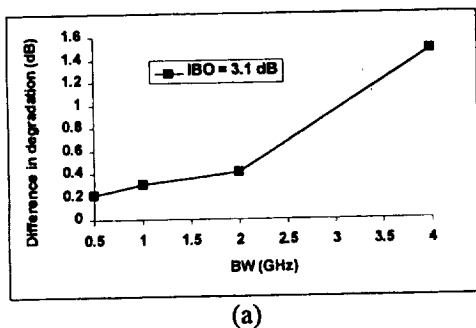

(a)

(b)

Figure 9 Difference in upper bound degradation using BPSK (a) 3.1 dB IBO, (b) BW = 2 GHz
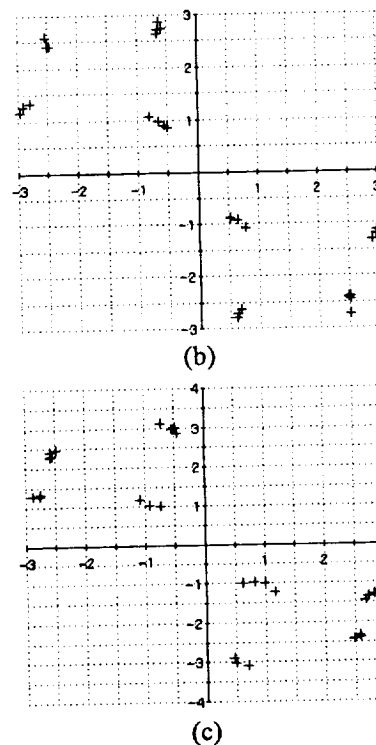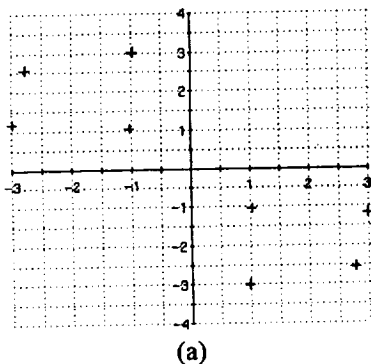

(a)

(b)

(c)

Figure 10 16-QAM constellation diagram (7.0 dB IBO) (a) SPW (2 and 4 GHz BWs), (b) MAFIA (2 GHz BW), and (c) MAFIA (4 GHz BW)

REFERENCES

1 SPW™, Signal Processing Worksystem. Comdisco Systems, Inc. 919 Hillsdale Blvd., Foster City, CA 94404

2 D. M. MacGregor, Two-dimensional nonlinear multisignal helix traveling-wave tube amplifier computer program, Volume 1: User Manual, Electrocon International, Inc., Ann Arbor, Michigan, April 1993

3 C. L. Kory, Three-dimensional simulations of PPM Focused Helical Traveling-wave tubes, Doctor of Engineering Dissertation, Cleveland State University, Cleveland, Ohio, August 2000..

4 T. Weiland, On the numerical solution of Maxwell's equations and applications in the field of accelerator physics, *Part. Accel.*, Vol. 15, pp. 245-292, 1984.

5 T. Weiland, On the unique numerical solution of Maxwellian eigenvalue problems in three dimensions, *Part. Accel.*, Vol. 17, pp. 227-242, 1985.

6 C. J. Clark, G. Chrisikos, M. S. Muha, A. A. Moulthrop and C. P. Silva, Time-domain envelope measurement technique with application to wideband power amplifier modeling, IEEE Trans. Microwave Theory and Techniques, Vol. 46, No. 12, Dec. 1998.

7 M. C. Jeruchim, P. Balaban, and K. S. Shanmugan, Simulation of Communication Systems. Modeling, Methodology, and Techniques, 2nd Edition, Kluwer Academic/Plenum Publishers, New York (2000).

8 J. W. Hansen, G. A. Lange, A. S. Rostad and R. L. Woods, Hughes Aircraft Company Electron Dynamics Division *Applications Note System Aspect of Communications TWTAs*, August 1982.

9 Andy Bateman, *Digital Communications- Design for the Real World*, Addison-Wesley, Edinburgh Gate, UK, 1999.